One-step synthesis of hierarchical pentasil zeolite microspheres using diamine with linear carbon chain as single template†

Li Chen, Shu Yan Zhu, Yi Meng Wang* and Ming-Yuan He

Received (in Montpellier, France) 27th April 2010, Accepted 18th June 2010
DOI: 10.1039/c0nj00316f

Hierarchical zeolite microspheres were synthesized *via* a one-step method using a diamine with a linear carbon chain as the single template, where no secondary template and additives were added. The obtained microspheres possessed significant textual porosity (up to 0.24 $cm^3\ g^{-1}$), which was tuneable by carefully choosing diamines with different length hydrocarbon chains and the amount of aluminium in the synthetic mixture. The zeolite microspheres not only possessed high activities in catalytic applications but also curtailed to some extent filtration difficulties in their preparation and application. During the hydrothermal synthesis, zeolite nanocrystals (50 nm) were formed and spontaneously assembled into uniform microspheres in size of 5–8 μm following a particle–particle aggregation mechanism.

Introduction

The discovery of zeolite ZSM-5 in 1963 by the former Mobil led to a new discipline in material science, catalysis, separation science, and petrochemical and organic chemistry.[1] These highly siliceous hydrophobic medium-pore zeolites have dominated the catalysis scene for more than 40 years and have great significance in the history of shape selective catalysis. Four different types of zeolite-based materials, including wide-pore zeolites, nanosized zeolites, mesoporous zeolite crystals and zeolite composites with zeolite crystals supported on mesoporous or macroporous materials, could offer improved accessibility to the catalytically active sites located in microporous crystals,[2,3] as the rate of intracrystalline transport could affect the reaction kinetics and product distribution. However, sometimes, large crystals of ZSM-5 must be used to achieve high *para*-selectivity.[4] Recently, hierarchical zeolites have proven to be a useful strategy for combining shape selectivity with efficient mass transport.[5] Some good reviews have summarized the methods used to prepare the hierarchical zeolites:[3–5] (1) the assembly of zeolite nanocrystals induced by latex spheres, cationic polymers, *in situ* polymerization and silanization, and others; (2) crystallization of zeolite precursors deposited on mesoporous supports or the walls of mesoporous materials; (3) post-treatment of zeolite crystals by steaming, and acid and base leaching; (4) crystallization *via* a double-template technique, including both mesogenous templates and zeolitic structure-directing templates, where the mesogenous template could be hard a template, including carbon, nanosized $CaCO_3$ and others, or a soft template, for example, amphiphilic organosilanes, *etc*. Unfortunately, most of this work still requires inorganic and organic templates to generate the mesopores or macropores.

Shanghai Key Laboratory of Green Chemistry and Chemical Processes, Department of Chemistry, East China Normal University, North Zhongshan Road 3663, Shanghai, 200062, China. E-mail: ymwang@chem.ecnu.edu.cn; Fax: +86 21 62232251
† Electronic supplementary information (ESI) available: Further experimental data. See DOI: 10.1039/c0nj00316f

Hayasaka *et al*. pointed out that ZSM-22 zeolite particles could be formed by the alignment and fusion of nanorods.[6] By learning from studies on the formation mechanism of zeolites carried out at a lower temperature, a particle–particle aggregation mechanism could be applicable for many zeolites, such as ZSM-5, ZSM-12, ZSM-22 and Beta zeolite.[6–8] Therefore, there are possibilities to synthesize hierarchical zeolites using a single template by exploiting the particle–particle aggregation mechanism. Recently, Chen reported that a mesoporous aggregate of zeolite nanocrystals can be synthesized without a secondary template by the self-assembly of *in situ*-formed zeolite nanocrystals.[7] Ryoo and co-workers showed that an appropriately designed bifunctional template[9] or cyclic diammonium[10,11] as a single template can simultaneously direct the formation of zeolite structures on mesoporous and microporous size scales. The generation of nanocrystalline products through these two different crystallization mechanisms indicates that the presence of two ammonium groups in the same molecule could be the most important factor for the generation of nanocrystalline morphologies and mesoporosity.[11] However, the obtained ZSM-5 zeolite consisted of large and irregular aggregates with sizes of only about 500 nm, which is still very difficult for separation and recovery. Therefore, it is highly desirable to synthesize nanocrystalline zeolite aggregates with tunable hierarchical pores without a secondary template, exhibiting high catalytic activity in the bulk molecular reaction and curtailing to some extent the filtration difficulties in their preparation.

Here, we report that mesoporous zeolite pentasil microspheres were successfully synthesized using diamines with linear carbon chains as single templates. During the hydrothermal synthesis, zeolite nanocrystals (50 nm) were formed and spontaneously assembled into uniform microspheres of 5–7 μm in size. The obtained microspheres possess a significant textual porosity (up to 0.24 $cm^3\ g^{-1}$), which is tuneable by carefully choosing diamines with different hydrocarbon chain lengths and the amount of aluminium in the synthetic mixture. These zeolite microspheres not only possess high activities in

catalytic applications, but also curtail the filtration difficulties in their preparation and application to some extent.

Results and discussion

XRD patterns of the mesoporous zeolite microspheres are given in Fig. 1. When the templates are EDA and HDA, the obtained samples with both SiO_2/Al_2O_3 ratios are all ZSM-5 zeolites with MFI structures, consistent with those reported in the literature.[12] However, with increasing linear chain length of the template, the as-made samples synthesized using DAOT and DADC as templates are highly crystalline ZSM-11 zeolites with MEL structures.[13] The XRD patterns of the characteristic peaks of ZSM-5 and ZSM-11 in the region of $2\theta = 44°–46°$ are shown in Fig. S1.† In general, the XRD peak at $2\theta \approx 45°$ was not split for ZSM-11, but was split for ZSM-5. The role of small amines in zeolite synthesis remains uncertain.[14] Davis and Lobo showed that at least 22 different organic molecules can be used to synthesize ZSM-5,[15] while one organic molecule, tetraethylammonium hydroxide, can lead to different zeolites, including ZSM-11, Beta and ZSM-12. Corma and Davis pointed out that the organic SDA should be somewhat rigid so that multiple configurations are not possible under synthesis conditions.[16] Here, the great flexibility of the linear chain makes the deformation of diamines possible, providing a good fit within the zeolite void space. Therefore, only zeolite pentasil, including ZSM-5 and ZSM-11, were obtained in our case. Rollmann *et al.* showed that ZSM-11 could be synthesized in the presence of one or more alkylenediamines having from 7 to 12 carbon atoms, which agrees with our results.[13]

The crystallization rate is affected by the amount of aluminium, the chain length of the diamine and other factors. In the case of HDA-ZSM-5-60, the relative crystallinity determined by XRD reached 45.4% when the crystallization time was 1 d. This crystallization rate is slightly faster that those in ref. 18 and ref. 19, where no crystalline phases were detected by XRD after 1 d. This fast crystallization rate may be attributed to the lower H_2O/SiO_2 ratio of 24 in the present work; the H_2O/SiO_2 ratios are 40 and 50, respectively, in the reports of Araya and Valtchev.[18,19] These relatively dilute systems result in slow crystallization rates, although the Na_2O/SiO_2 and R/SiO_2 ratios in those two papers are higher than those in the present work. Furthermore, the crystallization rate of HDA-ZSM-5-30 is slower than that of HDA-ZSM-5-60 (as shown in Fig. S2 and Table S1†), which illustrates that the crystallization rate can be affected by the amount of aluminium.[17] Moreover, the crystallization rate can be affected by the chain length of the diamine. The longer the chain length of the diamine the slower the crystallization rate. In case of DAOT and DADC, it took 10 d to obtain highly crystalline ZSM-11 zeolite, while well-formed zeolite ZSM-5 appeared only after 5 d in the presence of EDA and HDA. With the molar ratio of C/N in diamines increasing, the enhanced hydrophobicity reduces their solubility in aqueous synthetic mixtures and thus weakens their directing function to form zeolites. With the increase in linear chain length of the diamine or the amount of aluminium, the XRD patterns of zeolites show lower peak heights and wider half-peak widths, which indicates a reduction in the mean crystallite sizes of the materials as judged by the Scherrer equation. This result is in accordance with the conclusion reported by Cundy *et al.*,[20] who thought that under certain conditions, the ultimate particle size decreased with increasing aluminium concentration.

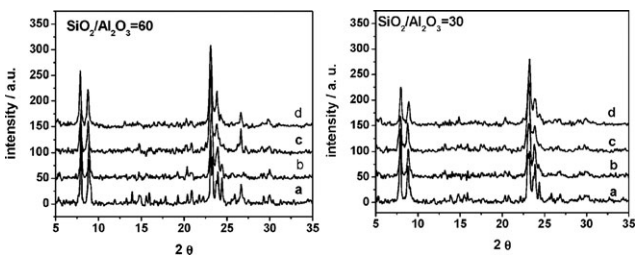

Fig. 1 Powder XRD patterns of the as-synthesized ZSM-5 microspheres with different SiO_2/Al_2O_3 ratios synthesized by (a) EDA, (b) HDA, (c) DAOT and (d) DADC templates at 428 K for (a) 5 d, (b) 5 d, (c) 10 d and (d) 10 d (b: *y*-axis shift: 50; c: *y*-axis shift: 100; d: *y*-axis shift: 150).

As shown in the SEM images (Fig. 2a and b), the resulting materials were both composed of relatively uniform spherical aggregates of 5–8 μm diameter. The insets are high magnification SEM images of a single microsphere, showing that the microspheres are aggregates of nanosized zeolite crystals with clearly defined grain boundaries. The size of HAD-ZSM-5-30 nanoparticles is about 50–100 nm (Fig. 2b, inset), much smaller than that of the HAD-ZSM-5-60 sample (Fig. 2a, inset). Moreover, the size of the crystallographic domains according to the Scherrer equation from XRD data is listed in Table S2.† Unfortunately, these data are not consistent with that from the SEM, for which there may be two reasons. Firstly, values for the coefficient K in the Scherrer equation depend on factors such as the geometry of the crystallites and are, unfortunately, not always consistently used in the literature. Moreover, the primary nanoparticles in spheric aggregates are not isolated, but intergrown or overlapped. There are some mismatched orientations in the spherical agglomerate according to TEM image in Fig. 2h and the corresponding SAED patterns.

With the length of the hydrophobic chain of the diamine increasing, nanosized crystals in the zeolite microsphere became smaller. Similarly, ZSM-11 microspheres (10 × 15 μm) with large intergrowth crystals could be synthesized by using 1,8-diaminooctane as the template.[21] These syntheses were carried out using potassium hydroxide as a mineralization agent, and no porosity data are given. Furthermore, different morphology pentasil zeolites could be synthesized by using various diamines as templates, which may be due to the different molar compositions of the synthetic mixtures, and the different nature and concentration of the starting materials.[22–26] However, the size of zeolite microspheres did not drastically change with varying diamine chain length. This relatively large aggregate size is a positive fact that favors easy recovery in their preparation and application. If all nanosized zeolites were isolated and highly dispersed, their filtration would be difficult due to their colloidal properties.

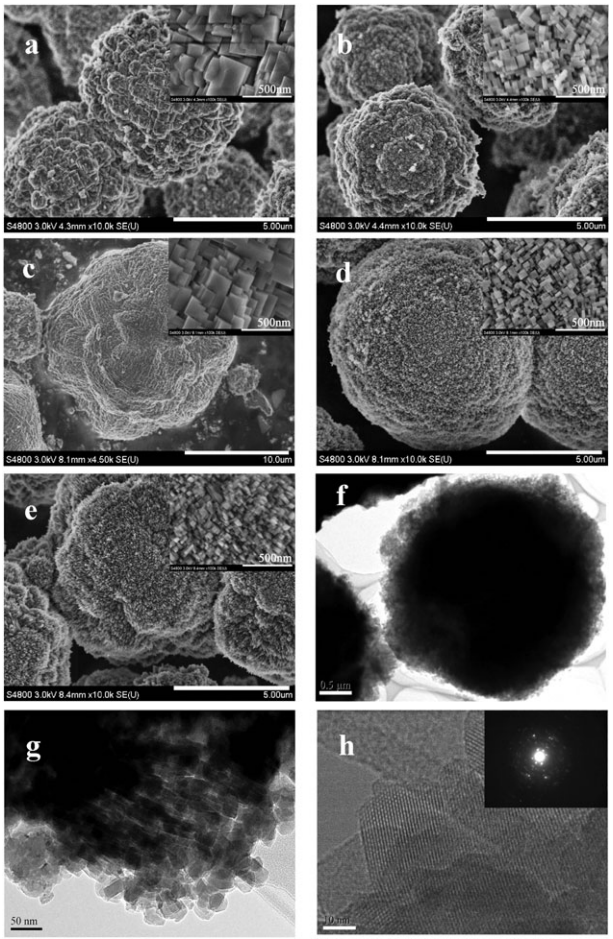

Fig. 2 SEM images of zeolite pentasil microspheres (a) HDA-ZSM-5-60, (b) HDA-ZSM-5-30, (c) EDA-ZSM-5-30, (d) DAOT-ZSM-11-30 and (e) DADC-ZSM-11-30. Inset is a high magnification SEM image of the microsphere surface of showing aggregated zeolite nanocrystals. (f) The TEM image of a single HDA-ZSM-5-30 microsphere. (g) and (h) High-resolution TEM images taken at the edge of a HDA-ZSM-5-30 microsphere.

The TEM image (Fig. 2f) shows a micrometre-sized particle with a spherical morphology. The high-resolution TEM image taken at the edge of the microsphere shows small grains with clear lattice fringes, confirming that the microsphere is made of zeolite nanocrystals rather than amorphous silica.

The effects of the Na_2O/SiO_2 and H_2O/SiO_2 ratios on the synthesis mixture are presented in the SEM images of Fig. 3. When the Na_2O/SiO_2 ratio ranged from 0.08 to 0.12, the size of the primary particles in the zeolite microspheres gradually reduced. However, the aggregates of particles retained a microspherical morphology and were of similar size. This may be because the diamine is a weak organic base and can act as a mineralizing agent in the synthesis mixtures, which makes the pH of the synthesis mixture slightly changeable. Thus, the uniformity of the charge density and polymerization of the silica species can be retained.[26] Furthermore, the morphology of HDA-ZSM-5-30 is affected by the H_2O/SiO_2 ratio. In case of a H_2O/SiO_2 ratio of 19, the aggregate of the particle size becomes much closer, and the shape of the zeolite aggregates change from microspheres to irregular

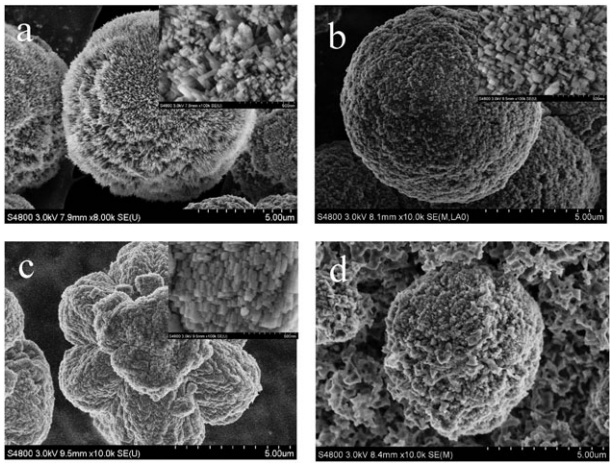

Fig. 3 SEM images of the as-synthesized HDA-ZSM-5-30 zeolites synthesized at 428 K for 5 d: (a) Na_2O/SiO_2 = 0.08, (b) Na_2O/SiO_2 = 0.12, (c) H_2O/SiO_2 = 19 and (d) H_2O/SiO_2 = 50.

blackberry-like aggregates of small nanoparticles. With the H_2O/SiO_2 ratio increasing up to 50, a decrease in alkalinity of the synthesis mixture results in a slower crystallization rate. As shown in Fig. S3,† the intensity of the characteristic diffraction peaks is low, and there is a strong amorphous bump, indicating the presence of amorphous silica in the sample. Therefore, more amorphous silica is present in the synthesis system after the same crystallization time by increasing in the molar ratio of H_2O/SiO_2.

Thermogravimetric (TG) analysis of the as-prepared zeolite microspheres was conducted in air. The TG plot showed three weight loss steps, with a total weight loss of 10–15% ranging from room temperature to 800 °C (Fig. S4†). The first step, appearing below 200 °C, was associated with the desorption of water. The second step, between 250 and 500 °C, might correspond to the decomposition of the diamine in the micropore. As shown in Fig. S1,† the decomposition temperature of the diamine in the micropore of the zeolite varied with the linear chain length. When the chain length of the diamine was C2–C6, the template was located in the *b* direction straight channel of ZSM-5[27] and the decomposition temperature was high. When the chain length of the diamine increases to C7–C10, the template is located in the straight pore channel of ZSM-11[28] and the decomposition temperature is low. The last step, between 500 and 800 °C, might correspond to dehydroxylation of the zeolite microspheres.

N_2 adsorption–desorption isotherms measured at 77 K are shown in Fig. 4, and the surface area, total volume and micropore volume data of all the samples with two different SiO_2/Al_2O_3 ratios are listed in Table 1. The isotherms are of type IV with hysteresis loops in the relative pressure range P/P_0 = 0.5–0.9, indicating the presence of irregular mesopores. The horizontal hysteresis loop could relate to some secondary porosity that is in contact with the exterior by channels of zeolite and is desorbing by cavitation. All the samples had similar micropore volumes of 0.12–0.13 $cm^3\ g^{-1}$, while the mesopore volume varied greatly from 0.06 to 0.20 $cm^3\ g^{-1}$. The samples HDA-ZSM-5-30 and DAOT-ZSM-11-30 had quite large mesopore volumes of 0.19–0.20 $cm^3\ g^{-1}$. These

results prove that alkylenediamines with medium carbon length chains as single templates could also lead to hierarchical zeolite spheres with large mesopore volumes. The BET surface area of these zeolite microspheres amounted to 313–369 m^2 g^{-1}, slightly higher than the hierarchical zeolite microspheres prepared by using F127 ($EO_{106}PO_{70}EO_{106}$) polymer as a secondary template[29] and slightly lower than the hierarchical ZSM-5 microspheres prepared in the presence of the urea-formaldehyde polymer.[30] The main difference may ascribed to the primary zeolite nanoparticles. As shown in the high magnification SEM images of Fig. 2, the primary zeolite nanoparticles in the microspheres templated by diamines are well faceted and intergrown, while the nanozeolites in the microspheres prepared with the urea-formaldehyde polymer are pre-formed, but show no well-defined crystal faces and randomly aggregate with each other. The high BET surface areas and large mesopore volumes of zeolites may favor the reaction of bulky molecules, resulting in a higher catalytic activity,[31] an excellent anti-coke formation ability and an anti-sulfur poisoning ability in catalytic reactions.[32,33]

Fig. S5A displays ^{27}Al NMR spectra of the zeolites synthesized by diamines with different linear chain lengths.†

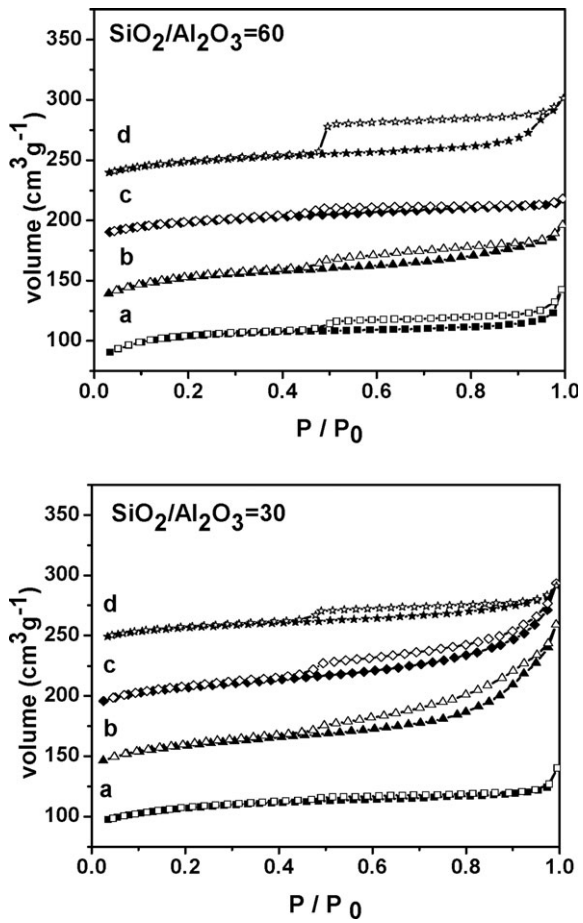

Fig. 4 Nitrogen adsorption–desorption isotherms of the calcined mesoporous zeolite microspheres with different SiO_2/Al_2O_3 ratios synthesized by (a) EDA, (b) HDA, (c) DAOT and (d) DADC templates at 428 K for (a) 5 d, (b) 5 d, (c) 10 d and (d) 10 d. The isotherms for samples (b), (c) and (d) are offset vertically by 50, 100 and 150 cm^3 g^{-1}, respectively.

In general, the resonance centered at 54 ppm is commonly assigned to four-coordinated framework aluminium, while the peak at 0 ppm is refers to non-framework octahedral aluminium. There is almost no peak at 0 ppm in any of the samples, indicating the absence of non-framework aluminium, no matter what diamine and SiO_2/Al_2O_3 ratio was used.

As shown in Fig. S5B,† the ^{29}Si MAS NMR spectra indicate a main peak at a chemical shift of *ca.* −114 ppm for Q_4 species with a shoulder centered at −106 ppm from Q_3 entities in all the samples. The Q_4/Q_3 ratio, calculated from the deconvoluted peaks (dashed lines), was 2.2 when the SiO_2/Al_2O_3 ratio was 30. When the SiO_2/Al_2O_3 ratio was increased to 60, the Q_4/Q_3 ratio calculated from the deconvoluted peaks changed to 6.5. The higher percentage of Q_3 entities in the samples with more alumina content indicates that mesoporous ZSM-5 has more hydroxyl groups and thus a more hydrophilic surface. Almost no Q_2 signals are observed in either spectrum, suggesting a high degree of condensation of the framework in the zeolites.

Accordingly, the SEM images and IR spectra of DAOT-ZSM-11-30 prepared for different crystallization times of (a) 3 d, (b) 5 d, (c) 7 d and (d) 10 d are shown in Fig. 5. As shown in the SEM images, there are some irregularly-shaped gel lumps at early stages of the hydrothermal reaction (3 d). After 5 d, some microspheres are randomly dispersed in the amorphous gel, as shown in Fig. 5B, while no crystalline zeolite is observed by XRD (not shown). However, a small band at 550 cm^{-1} appears in the IR spectrum. With the crystallization time increased to 7 d, more and more irregularly-shaped gels transform into microspheres with diameters of ~5 μm. Meanwhile, the band at 550 cm^{-1} becomes larger and no well-crystallized zeolites are seen by XRD. After 10 d, almost all the amorphous gel has disappeared, well-crystallized zeolite ZSM-11 microspheres of 5–7 μm in diameter have formed and the band at 550 cm^{-1} becomes distinct. The band at 550 cm^{-1} is characteristic of MFI/MEL zeolites with five-membered rings.[34–37] The intensity ratio of the 550 and 450 cm^{-1} bands has been used to assess the formation of ZSM-11 and has been named IR crystallinity. The band at 550 cm^{-1} grows stronger and sharper gradually as the crystallization time is prolonged. As indicating by all the SEM images and IR spectra with varied crystallization times, the formation of a macroscopic morphology and a zeolitic framework seem to occur simultaneously.

The liquid alkylation of phenol with *tert*-butyl alcohol is a typical Friedel–Crafts alkylation that can be catalyzed by acid catalysts. The different acid sites and pore structures lead to different distributions of products.[38–40] The catalytic activities of ZSM-5-ind and zeolite microspheres synthesized by diamines in the alkylation of phenol and *tert*-butyl alcohol are listed in Table 2. Industrial ZSM-5-30 had a very low catalytic activity, where phenol conversion was only 4.92%. In contrast, the zeolite microspheres exhibited much higher catalytic activities, with phenol conversion reaching 6.6–19.5% under the same reaction conditions. The catalytic activity of HDA-ZSM-5-30 was nearly three times higher that of ZSM-5-ind and similar to that of a reported mesoporous ZSM-5 synthesized by a carbon template.[41] The increase of activity could mainly be attributed to a reduction in the

Table 1 The textual properties of the mesoporous zeolite samples

Samples	S_{BET}/m^2 g^{-1} [a]	V_{pore}/cm^3 g^{-1} [b]	$V_{micropore}$/cm^3 g^{-1} [c]	$V_{mesopore}$/cm^3 g^{-1}	$S_{external}$/m^2 g^{-1}
EDA-ZSM-5-60	320	0.21	0.12	0.09	101
HDA-ZSM-5-60	369	0.25	0.13	0.12	114
DAOT-ZSM-11-60	318	0.19	0.13	0.06	76
DADC-ZSM-11-60	315	0.24	0.12	0.12	81
EDA-ZSM-5-30	327	0.22	0.13	0.09	87
HDA-ZSM-5-30	355	0.33	0.13	0.20	109
DAOT-ZSM-11-30	330	0.30	0.12	0.18	99
DADC-ZSM-11-30	321	0.22	0.13	0.09	71

[a] S_{BET}: apparent surface area calculated by the BET method. [b] V_{pore}: total pore volume at $P/P_0 = 0.99$. [c] $V_{micropore}$: micropore volume calculated by the *t*-plot method.

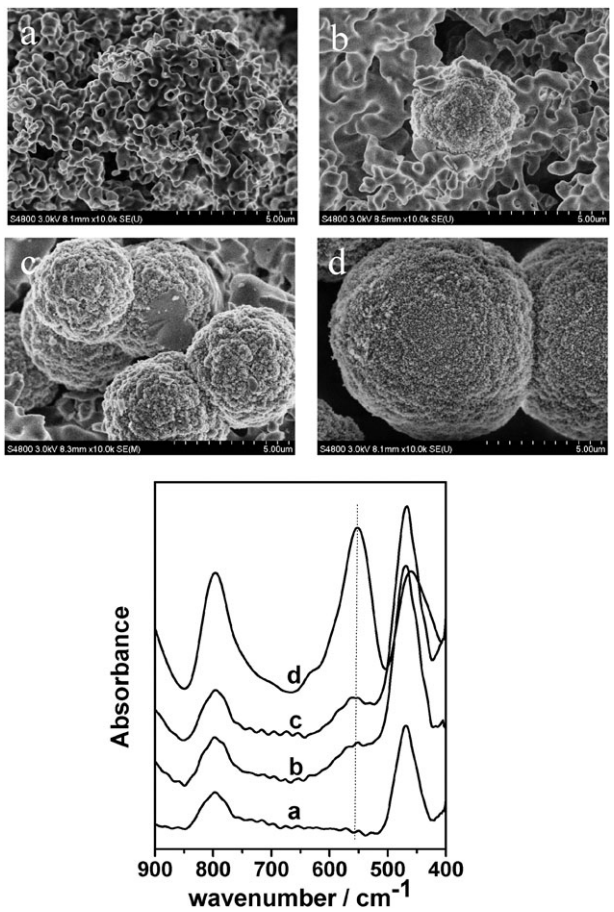

Fig. 5 SEM and IR spectra of DAOT-ZSM-11-30 with the crystallization times of (a) 3 d, (b) 5 d, (c) 7 d and (d) 10 d.

diffusion limitation because of a decrease in the size of the zeolite crystals and also the presence of secondary porosity. As shown in Fig. S6,† the ZSM-5-ind sample contains the aggregation of crystals ranging from 0.2 to 1.5 μm, which is larger than those in the microspheres. Therefore, the low catalytic activity of ZSM-5-ind can mainly be ascribed to slow diffusion in larger crystals. Furthermore, DAOT-ZSM-11-30 and DADC-ZSM-11-30 samples showed lower phenol conversions than EDA-ZSM-5-30 and HAD-ZSM-5-30, as shown in Table 2, although the former two samples have smaller sizes of their primary zeolite nanoparticles. The reason for this may be attributed to the different topological structure of the zeolite catalyst. At the same SiO_2/Al_2O_3 ratio, the higher catalytic activity of HDA-ZSM-5-30 is due to its higher mesoporous volume, indicating that the existence of mesopores assembled by nanoparticles greatly overcomes the diffusion limitation. Moreover, the large size of the zeolite microspheres may to some extent curtail the filtration difficulties in their preparation and catalytic application.

Here, zeolite pentasil microspheres with mesoporosity could be synthesized by using linear diamines as single templates. This synthesis method is very simple and easy compared to mesoporous ZSM-5 synthesized by a carbon template,[41] and all the templates used here are commercially available. Most importantly, diamines with medium linear carbon chains not only direct the formation of the crystalline zeolite structure but also favor control of the macroscopic morphology and tectonics of the zeolite crystals. These results prove that non-amphiphilic organic molecules could also lead to hierarchical zeolites with both micro- and mesoporosity *via* a single hydrothermal treatment. Furthermore, zeolite microspheres with mesoporosity could not only reduce diffusion limitations in catalytic reactions but also curtail the recovery difficulties in their preparation and application.

Conclusions

A facile one-step method has been developed for the preparation of mesoporous zeolite microspheres using linear diamine templates. During the hydrothermal crystallization, zeolite nanocrystals (50 nm) were formed and spontaneously assembled into uniform microspheres of 5–8 μm in size. The obtained microspheres possess a significant textual porosity (up to 0.24 cm^3 g^{-1}) that is tunable by simply adding different hydrocarbon chains of the diamine and varying the amount of aluminium in the synthesis solution. The zeolite microspheres are useful for catalytic applications and may curtail to some extent the filtration difficulties in their preparation.

Experimental

Synthesis of hierarchical pentasil zeolite microspheres

Mesoporous pentasil zeolite materials were hydrothermally synthesized as follows. A solution of $Al_2(SO_4)_3{\cdot}18H_2O$ dissolved in an aqueous HCl solution was added dropwise to

Table 2 Catalytic activity and product distribution for the alkylation reaction of phenol with *tert*-butanol[a]

Catalyst[b]	SiO_2/Al_2O_3 ratio in the product	Phenol conversion (mol%)	Product distribution (mol%)		
			2-TBP	4-TBP	2,4-di-TBP
ZSM-5-ind	32.5	4.92	11.2	84.4	4.43
EDA-ZSM-5-30	25.0	11.8	19.9	60.3	19.8
HDA-ZSM-5-30	25.2	19.5	17.9	78.9	4.2
DAOT-ZSM-11-30	26.0	11.2	22.9	66.7	10.4
DADC-ZSM-11-30	25.0	13.8	5.9	79.2	14.9
HDA-ZSM-5-60	45.6	8.4	11.8	84.3	3.9

[a] Reaction conditions: 100 °C, 4 h, 0.15 g of catalyst, 7.78 g of cyclohexane, 0.74 g of *tert*-butanol, 0.47 g of phenol. [b] All the samples used in the catalytic reaction are their H-form.

an aqueous solution of $Na_2SiO_3 \cdot 9H_2O$, which was kept stirring until the pH value was lowered to 8. The freshly precipitated alumino-silica was recovered by filtration after being continuously stirred for 2 h. Subsequently ,the obtained solid was added to H_2O and the required diamine template (such as ethylenediamine (EDA), hexanediamine (HDA), 1,8-diaminooctane (DAOT) and 1,10-diaminodecane (DADC)). The molar composition of the synthetic mixtures was $60SiO_2 : xAl_2O_3 : 6Na_2O : 1440H_2O : 8.4$ diamine, where x = 1 and 2, respectively. After being stirred for 2 h, the mixtures were transferred into a Teflon-lined stainless steel autoclave, where they were heated statically under autogenous pressure for the prescribed time at 448 K. The products obtained were filtered, washed and then dried overnight at 373 K. The obtained samples were denoted X-Y-Z, where X is the name of template, Y is the zeolite name and Z refers to the SiO_2/Al_2O_3 ratio. The organic component was removed by calcination in air at 823 K for 6 h. Ion exchange was carried out four times with a 0.6 M NH_4NO_3 solution at 353 K, each for 1 h, followed by calcination at 823 K in air for 6 h to give the H-form products.

Characterization

The particle sizes and morphology of the mesoporous zeolite microspheres were characterized by scanning electron microscopy (type Hitachi S-4800) with an accelerating voltage of 3 kV. Transmission electron microscopy (TEM) characterization was carried on a JEM-2010 instrument operating at 200 kV. For the TEM images, the specimens were dispersed in ethanol and placed on holey copper grids. Powder X-ray diffraction patterns (XRD) of as-synthesized samples were obtained by a Bruker D8 Advance powder diffractometer using Cu-K_α radiation (K_α = 0.154184 nm) over a 2θ range from 5 to 35°; the accelerating voltage and applied current were 40 kV and 40 mA, respectively. Nitrogen adsorption–desorption measurements were carried at 77 K on a nitrogen adsorption apparatus (Quantachrome Autosorb-3B). The Brunauer–Emmett–Teller (BET) method was utilized to calculate the specific surface areas (S_{BET}) using adsorption data in a relative pressure range from 0.04 to 0.2. The total pore volume was estimated from the amount of nitrogen adsorbed at a relative pressure (P/P_0) of 0.99, and the micropore volume was calculated from the *t*-plot. ^{29}Si solid-state MAS NMR spectra were recorded on a Bruker DSX300 spectrometer and IR spectra were characterized by SpectrumTM GX.

Acknowledgements

This work was financially supported by the National Science Foundation of China (projects 20873042 and 20890122) and the Shanghai Leading Academic Discipline Project (Project B409). L. C. is thankful for the PhD Program Scholarship Fund of ECNU 2009 (Project 2009014).

References

1 W. Vermeiren and J. P. Gilson, *Top. Catal.*, 2009, **52**, 1131.
2 Y. S. Tao, H. Kanoh, L. Abrams and K. Kaneko, *Chem. Rev.*, 2006, **106**, 896.
3 J. Pérez-Ramírez, C. H. Christensen, K. Egeblad, C. H. Christensen and J. C. Groene, *Chem. Soc. Rev.*, 2008, **37**, 2530.
4 N. Y. Chen, *Ind. Eng. Chem. Res.*, 2001, **40**, 4157.
5 M. Hartmann, *Angew. Chem., Int. Ed.*, 2004, **43**, 5880.
6 K. Hayasaka, D. Liang, W. Huybrechts, B. R. De Waele, K. J. Houthoofd and P. Eloy *et al.*, *Chem.–Eur. J.*, 2007, **13**, 10070.
7 Y. M. Fang, H. Q. Hu and G. H. Chen, *Chem. Mater.*, 2008, **20**, 1670.
8 N. D. Hould and R. F. Lobo, *Chem. Mater.*, 2008, **20**, 5807.
9 M. Choi, K. Na, J. Kim, Y. Sakamoto, O. Terasaki and R. Ryoo, *Nature*, 2009, **461**, 246.
10 K. Na, M. Choi and R. Ryoo, *Chem. Commun.*, 2009, 2845.
11 K. Na, M. Choi and R. Ryoo, *J. Mater. Chem.*, 2009, **19**, 6713.
12 A. E. Persson, B. J. Schoeman, J. Sterte and J. E. Otterstedt, *Zeolites*, 1995, **15**, 611.
13 L. D. Rollmann and E. W. Valyocsik, USP 4,108,881, 1978.
14 L. D. Rollmann, J. L. Schlenker, S. L. Lawton, C. L. Kennedy, G. J. Kennedy and D. J. Doren, *J. Phys. Chem. B*, 1999, **103**, 7175.
15 M. E. Davis and R. F. Lobo, *Chem. Mater.*, 1992, **4**, 756.
16 A. Corma and M. E. Davis, *ChemPhysChem*, 2004, **5**, 304.
17 J. Aguado, D. P. Serrano, J. M. Escola and J. M. Rodriguez, *Microporous Mesoporous Mater.*, 2004, **75**, 41.
18 A. Araya and B. M. Lowe, *Zeolites*, 1986, **6**, 111.
19 S. Mintova and V. Valtchev, *Zeolites*, 1993, **13**, 299.
20 C. S. Cundy, B. M. Lowe and D. M. Sinclair, *Faraday Discuss.*, 1993, **95**, 235.
21 M. Derewinski and M. Machowska, *Stud. Surf. Sci. Catal.*, 2004, **154**, 349.
22 Z. Gabelica, M. C. Bierman, P. Bodart, A. Gourgue and J. B. Nagy, *Stud. Surf. Sci. Catal.*, 1985, **24**, 55.
23 S. Schwarz, M. Kojima and C. T. O'Connor, *Appl. Catal.*, 1991, **73**, 313.
24 N. Venkatathri, *Orient. J. Chem.*, 2005, **21**, 195.
25 R. Kawase, A. Iida, Y. Kubota, K. Komura, Y. Sugi, K. Oyama and H. Itoh, *Ind. Eng. Chem. Res.*, 2007, **46**, 1091.
26 W. Y. Lin, Q. Cai, W. Q. Pang, Y. Yue and B. S. Zou, *Microporous Mesoporous Mater.*, 1999, **33**, 187.
27 E. de Vos Burchart, J. C. Jansen, B. van de Graaf and H. van Bekkum, *Zeolites*, 1993, **13**, 216.
28 G. González, W. Stracke, Z. Lopez, U. Keller, A. Ricker and R. Reichelt, *Microsc. Microanal.*, 2004, **10**, 224.
29 J. Hua and Y. Han, *Chem. Mater.*, 2009, **21**, 2344.

30 Y. J. Kang, W. Shan, J. Y. Wu, Y. H. Zhang, X. Y. Wang, W. L. Yang and Y. Tang, *Chem. Mater.*, 2006, **18**, 1861.
31 V. N. Shetti, J. Kim, R. Srivastava, M. Choi and R. Ryoo, *J. Catal.*, 2008, **254**, 296.
32 S. Y. Sang, F. X. Chang, Z. M. Liu, C. Q. He, Y. L. He and L. Xu, *Catal. Today*, 2004, **93–95**, 729.
33 R. Van Grieken, J. L. Sotelo, J. M. Menendez and J. A. Melero, *Microporous Mesoporous Mater.*, 2000, **39**, 135.
34 P. A. Jacobs, H. K. Beyer and J. Valyon, *Zeolites*, 1981, **1**, 161.
35 J. C. Jansen, F. J. van der Gaag and H. van Bekkum, *Zeolites*, 1984, **4**, 369.
36 G. Coudurier, C. Naccache and J. C. Vedrine, *J. Chem. Soc., Chem. Commun.*, 1982, 1413.
37 M. B. Yue, L. B. Sun, T. T. Zhuang, X. Dong, Y. Chun and J. H. Zhu, *J. Mater. Chem.*, 2008, **18**, 2044.
38 J. Huang, G. Li, S. Wu, H. Wang, L. Xing, K. Song, T. Wu and Q. Kan, *J. Mater. Chem.*, 2005, **15**, 1055.
39 J. Huang, L. Xing, H. Wang, G. Li, S. Wu, T. Wu and Q. Kan, *J. Mol. Catal. A: Chem.*, 2006, **259**, 84.
40 Y. Y. Sun and R. Prins, *Appl. Catal., A*, 2008, **336**, 11.
41 K. Song, J. Q. Guan, S. J. Wu and Q. B. Kan, *Catal. Commun.*, 2009, **10**, 631.

